Applied Materials Today 39 (2024) 102348

Contents lists available at ScienceDirect

Applied Materials Today

journal homepage: www.elsevier.com/locate/apmt

Lyophilization of biomimetic amyloids preserves their regulatable, endocrine-like functions for nanoparticle release

Marianna TP Favaro [a,1,*], Hèctor López-Laguna [a,b,1], Eric Voltà-Durán [a,b], Lorena Alba-Castellon [b,c,g], Julieta M. Sánchez [a,b,d,e], Isolda Casanova [b,c,g], Ugutz Unzueta [b,c,g], Ramón Mangues [b,c,g], Antonio Villaverde [a,b,f,*], Esther Vázquez [a,b,f]

[a] Institut de Biotecnologia i de Biomedicina, Universitat Autònoma de Barcelona, 08193 Bellaterra, Spain
[b] CIBER de Bioingeniería, Biomateriales y Nanomedicina (CIBER-BBN, ISCIII), Universitat Autònoma de Barcelona, 08193 Bellaterra, Spain
[c] Institut de Recerca Sant Pau (IR SANT PAU), Sant Quintí 77-79, 08041 Barcelona, Spain
[d] Departamento de Química, Cátedra de Química Biológica, Facultad de Ciencias Exactas, Físicas y Naturales, ICTA, Universidad Nacional de Córdoba, Av. Vélez Sársfield 1611, Córdoba 5016, Argentina
[e] Instituto de Investigaciones Biológicas y Tecnológicas (IIByT), CONICET-Universidad Nacional de Córdoba, Córdoba 5016, Argentina
[f] Departament de Genètica i de Microbiologia, Universitat Autònoma de Barcelona, 08193 Bellaterra, Spain
[g] Josep Carreras Leukaemia Research Institute, 08025 Barcelona, Spain

ARTICLE INFO

Keywords:
Functional amyloids
Recombinant proteins
Dynamic protein depots
Endocrine-like function
Drug delivery

ABSTRACT

The secretory granules from the mammalian endocrine system are functional amyloids that act as dynamic depots to store and release protein hormones into the bloodstream. The controlled in vitro coordination between divalent cations and solvent-exposed histidine residues triggers reversible, cross-molecular interactions that result in granular protein aggregates with protein-leaking properties. While these synthetic particles are mechanically stable, they progressively disintegrate and release their protein building blocks, mimicking the performance of secretory granules. Envisaged as delivery systems for endocrine-like, time-sustained protein release, their clinical applicability should be supported by robust storage procedures, so far unset. Being lyophilization a desirable storage method for protein drugs, how this procedure could preserve the performance of clinically oriented functional amyloids is a neglected issue. We have here explored, tailored and validated lyophilization as an industrially and clinically friendly, fully scalable approach to the storage of functional amyloids aimed at secretion of protein-only nanoparticles. By doing so, protein-protein interactions in such materials have been characterized, and citrate identified as an efficient modulator of the temporal secretion profile, through which the sustainability of the leaking process can be finely regulated.

1. Introduction

A foremost topic in drug discovery is the development of systems and biocompatible materials to support efficient drug delivery [1–10]. Innovative platforms for the sustained release of bioactive molecules are particularly in demand to reach and maintain steady drug levels in chronic conditions with a minimal number of administration actions [11,12]. Looking into nature, non-toxic functional amyloids are protein materials widely distributed in all types of living beings, exhibiting numerous regulatory and structural roles [13–20]. Among them, secretory granules from the mammalian endocrine system are interesting models of prolonged protein delivery since, in the body, they ensure the right levels of required hormones in the blood [21–23]. These particles, which occur at the sub-micron scale [24], are self-organized as granular protein materials enriched in cross-beta-sheet amyloidal structure, which ensures cross-molecular interactions that involved defined protein patches among the full primary sequence [25]. Protein oligomerization in secretory granules is supported by reversible interactions between histidine residues in the polypeptide chains and ionic Zinc (Zn^{+2}) [26,27]. The ion-based architectonic nature of the secretory granules, although not completely understood, allows the time-prolonged detachment and release of the forming peptidic or

* Corresponding authors.
E-mail addresses: Marianna.Teixeira@uab.cat (M. TP Favaro), Antoni.Villaverde@uab.es (A. Villaverde).
[1] Equally contributed.

https://doi.org/10.1016/j.apmt.2024.102348
Received 13 June 2024; Received in revised form 17 July 2024; Accepted 17 July 2024
Available online 25 July 2024

protein hormones [22,28,29], probably by the displacement or chelation of Zn [28]. Therefore, compared to the administration of soluble protein drugs in clinics, that result in undesired peak and valley drug level oscillations [30–32], the application of biocompatible, slow-release protein depots with such amyloidal architecture offers a possibility to approach steady drug levels with minimal administration actions. In this regard, mechanistically recreating the Zn-mediated protein self-assembling (as artificial, granular amyloid materials) and self-disassembling as functional forms, ready for their biological function, might generate, in vitro, biologically friendly dynamic protein depots responsive to media conditions that could be applied in clinical settings as protein drug reservoirs.

Following this reasoning, we had previously developed fully biocompatible, non-toxic amyloids, microscale mimetics of secretory granules, by divalent cation-mediated in vitro aggregation of his-tagged proteins under laboratory conditions [33,34]. This is achieved through the controlled stoichiometric coordination of ions with the imidazole ring in histidine residues from solvent-exposed hexahistidine (H6) tags, through a simple mixing approach [35]. Like natural endocrine granules, these synthetic versions, at the microscale, maintain an amyloidal architecture and show the capability to allow a time-prolonged release of the forming protein to the bloodstream from subcutaneous implants [33]. Several cations, within the recommended dietary doses, have been assessed for fabrication, including Zn^{2+}, Ca^{2+}, Mg^{2+}, Fe^{2+} and Mn^{2+} [36]. By testing this approach with a diversity of therapeutic proteins, in vitro but also in animal models, these artificial secretory granules have been fully validated as highly efficient and promising platforms for the sustained release of cytotoxic proteins in oncology [33,37,38], immunogens in vaccinology [39], growth factors in regenerative medicine [40] and antimicrobial peptides [41] in infectiology. The successful data in all these fields, using a diversity of proteins and peptides, confirm the system as a slow-delivery platform with high versatility and transversal clinical applicability.

The route towards clinical development is supported by the fact that in this type of protein depots, polypeptides are not entrapped in any chemically heterogeneous holding matrix but self-contained in a granular structure that will further disintegrate, releasing their functional building block protein components. The compositional simplicity and chemical homogeneity are conditions highly convenient regarding the clinical implementation of the platform. A further requisite would be the availability of convenient storage conditions that enable high product stability, and easy and simple manipulation during administration [42–46]. In this regard, lyophilization is a preferred method for the storage of protein drugs [46–50], but its utility and possible impact on the performance of functional amyloids, during preparative formulations, have never been tested. Lyophilization of pathogenic amyloids for their biophysical characterization modifies their structural properties [51–53], an observation that might represent a problem regarding the application of this method to equivalent druggable materials. In general, challenges faced when approaching lyophilization of a new drug include the buffer choice but also the optimization of the final formulation [54]. The catalogue of available buffers offers a range of options regarding pH and ionic strength, parameters that are pivotal when considering protein stability during the freeze-drying process [55]. In comparison with phosphate and acetate buffers, the versatility of citrate buffer regarding the wide working pH range makes it very attractive [56]. However, its chelating properties observed under a diversity of molecular environments [57–60] and the consequent potential interactions of citrate with the coordinated metal ions pose concerns about the stability and performance of Zn-assisted protein clusters. Apart from the generic need of balancing stability, solubility, and compatibility with a particular polypeptide, lyophilization of functional amyloids should orbit around preserving the reversible stability of the metal-mediated cross-protein interactions that allow the endocrine-like functions for which these

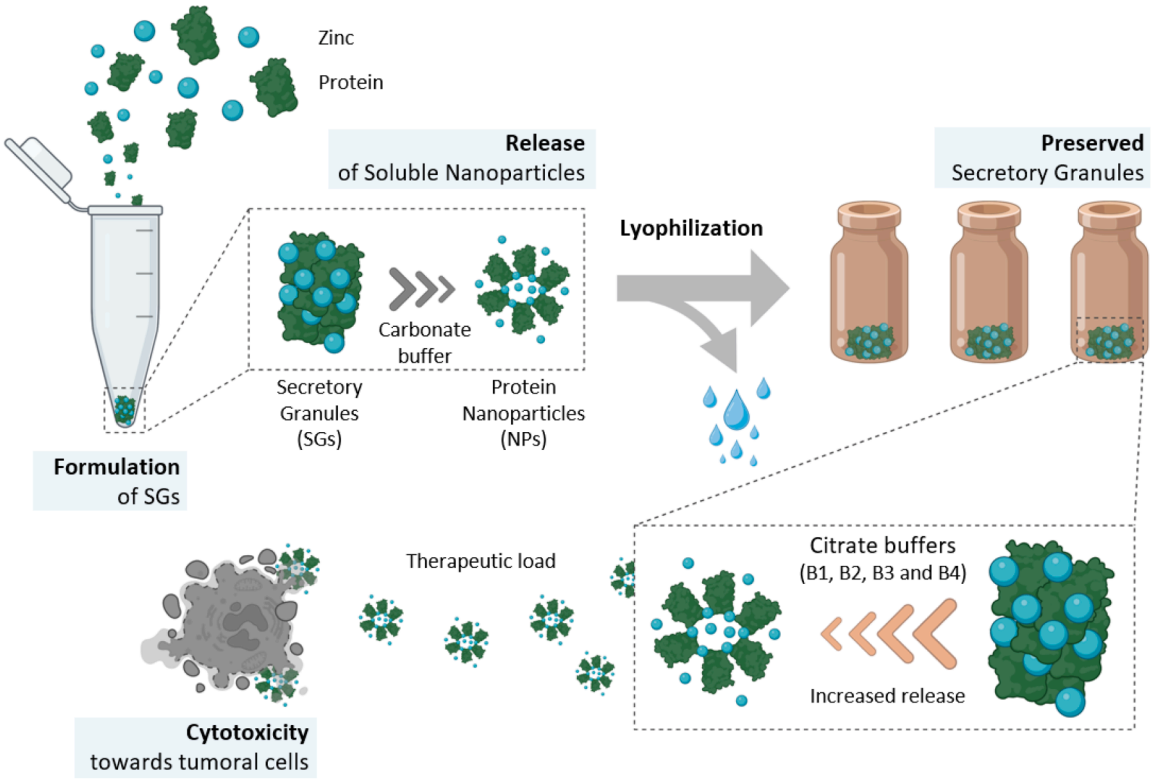

Fig. 1. A schematic illustration depicting the whole picture of this study. Cytotoxic protein nanodrugs of interest in oncology, prepared as amyloidal, endocrine-mimetic secretory granules, have been used as models to explore lyophilization protocols. Several citrate buffers (namely B1, B2, B3 and B4, see the composition in Figure 3) have been explored for lyophilization. The resulting reconstituted materials have been assessed regarding structure and cytotoxic activity over target cancer cells.

emerging materials are valuable. In the present study (Fig. 1), and by using receptor-targeted antitumoral drugs as models, we have deeply explored how lyophilization protocols and the composition of the lyophilization buffer, focusing on citrate, can be adapted to the storage of synthetic secretory granules. Also, we have investigated how the endocrine-like, protein leakage function can be maintained or even improved in the resulting material. In addition, the obtained results provide intriguing clues to understand the intricate molecular environment of the proteins within the secretory protein platform and its adaptation for high bioavailability, functionality and efficient and regulatable time-prolonged release of the embedded protein.

2. Experimental section

2.1. Materials

Gene constructions were purchased from Geneart (ThermoFisher). The protease inhibitor cOmplete was purchased from Roche. IMAC

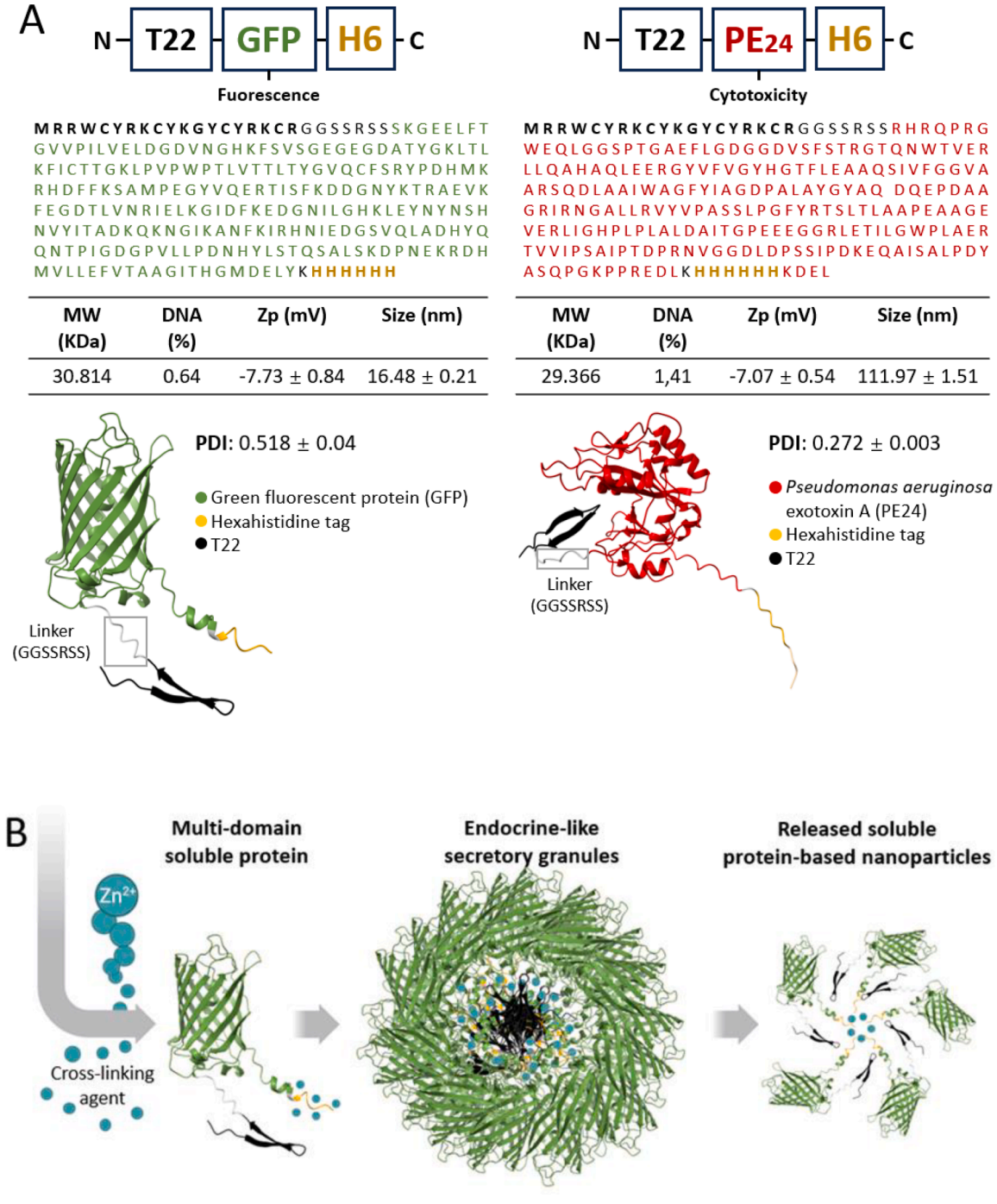

Fig. 2. Protein description and formation of secretory microgranules. (A) Protein sequence and corresponding structure of the modular T22-GFP-H6 and T22-PE24-H6, highlighting the harbored functional peptides. The Polydispersion index (PDI) is also displayed. The table indicates the molecular weight (MW), the percentage of double strand DNA (dsDNA) content, Zeta potential (Zp) and hydrodynamic size (measured by DLS) of each protein upon purification. (B) Schematic representation of the Zinc-mediated formation of secretory microgranules. The addition of ionic Zinc as a cross-linking reagent to either soluble proteins or oligomeric nanoparticles generates amyloidal endocrine-like secretory granules that slowly release the forming protein as oligomeric nanoparticles.

columns were supplied by Cytiva. For buffer preparation, we acquired Tris and NaCl from Fisher, Sodium bicarbonate from Sigma, and Imidazole from Millipore. Bradford reagent was purchased from Biorad. Cell culture medium and supplements (MEM Alpha GlutaMAX medium, RPMI 1640 medium, FBS, StrepPen, Trypsin-EDTA, Glutamine and Dulbecco's Modified medium) were purchased from Gibco, while the MTT reagents were purchased from Promega and Roche diagnostics. Cell lines cell lines HeLa (ATCC—CCL-2) and Toledo ATCC—CRL-

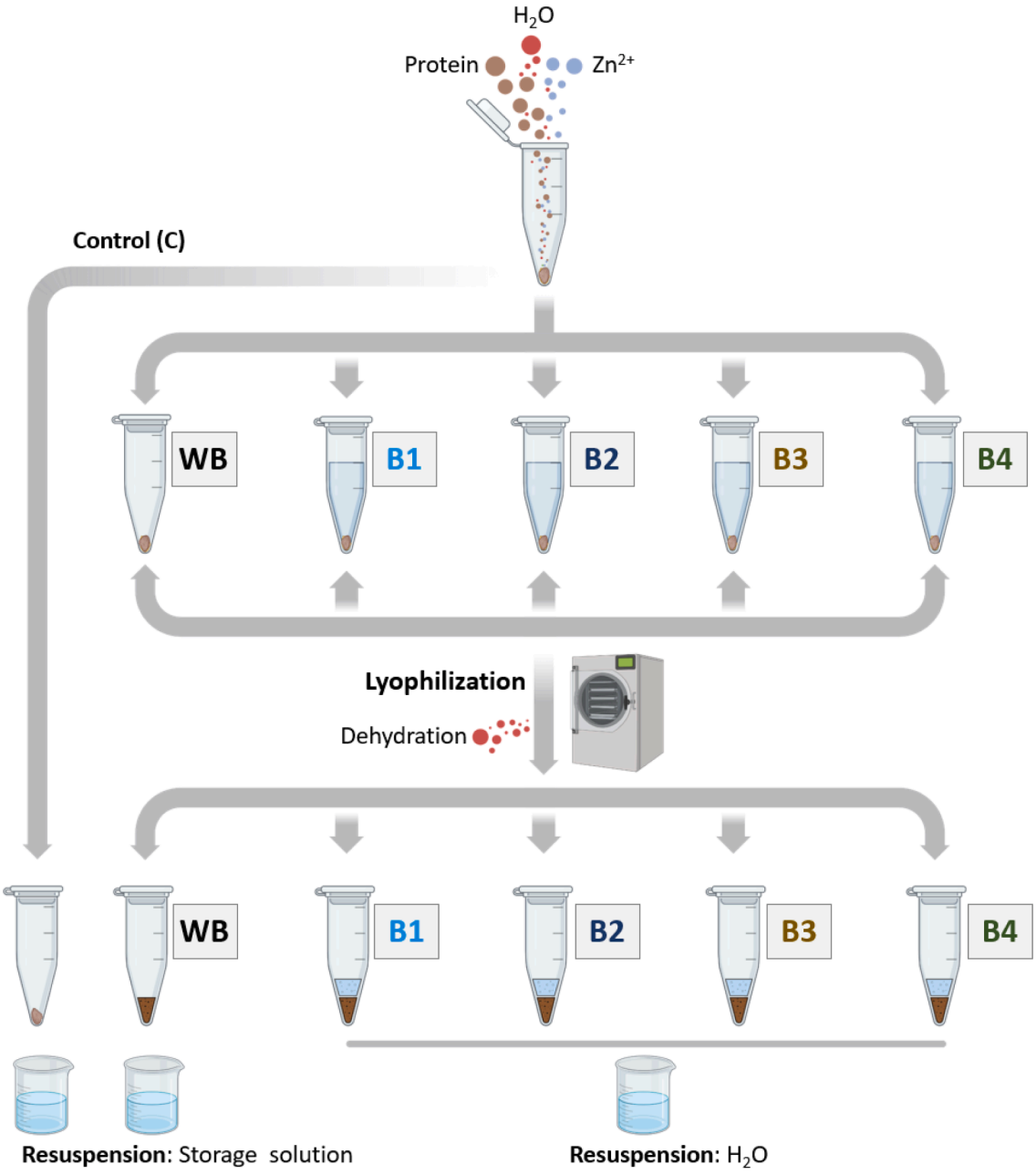

Control	WB	B1	B2	B3	B4
Storage solution	Storage solution	20 mM Citrate pH 6 4 % Trehalose	20 mM Citrate pH 6 4 % Trehalose 0.01 % Polysorbate 80	20 mM Citrate pH 6 8 % Trehalose 0.01 % Polysorbate 80	20 mM Citrate pH 6 6 % Trehalose 0.04 % Polysorbate 80

Fig. 3. Lyophilization steps and buffer evaluation in downstream processing of secretory microgranules. All secretory granules were prepared following a standard protocol. Except for control granules (C), the others were lyophilized without any further preparation (WB – lyophilized without any buffer) or after being briefly resuspended in buffers 1–4. After complete lyophilization, granules were resuspended in the original protein storage solution (for samples C and WB), or in water (for samples B1-B4 that already contained the original buffer elements). The table summarizes the final buffer condition where granules are in all downstream applications. WB refers to secretory granules lyophilized without the presence of any solution and subsequently resuspended with a storage solution. C refers to secretory granules directly resuspended with a storage solution without undergoing lyophilization.

2631™) were acquired from ATCC, while UM-SSC-22A-CXCR4^{+} was provided by Dr. Gregory Oakley and subsequently transfected with CXCR4-Luciferase lentiviral plasmid [61].

2.2. Protein production and purification

Genes encoding the modular proteins T22-GFP-H6 and T22-PE24-H6 (Fig. 2) were designed in-house and provided by Geneart as *Escherichia coli* codon-optimized genes hosted in a pET22b plasmid. All plasmids were transformed, and recombinant proteins produced in *E. coli* Origami B (BL21, OmpT^{-}, Lon^{-}, TrxB, Gor^{-}; Novagen) at 20 °C overnight upon induction of gene expression with 0.1 mM of Isopropyl-β-d-thio-galactopyronaside (IPTG). Bacterial cultures were harvested by centrifugation (15 min, 5000 x g) and resuspended in Wash buffer (20 mM Tris, 500 mM NaCl, 10 mM Imidazole, pH 8) in the presence of protease inhibitors (cOmplete EDTA-Free, Roche). Cells were disrupted by three rounds of disruption (Emulsiflex-C5—Homogenizer; Avestin) at 500–1000 psi and the soluble fraction was separated by centrifugation (45 min, 15.000 x g). Purification was performed by Immobilized Metal Affinity Chromatography (IMAC) using HiTrap Chelating HP 5 mL columns in an ÄKTA pure system (GE Healthcare). Elution was achieved by a linear gradient of elution buffer (20 mM Tris, 500 mM NaCl, 500 mM Imidazole, pH 8) and eluted proteins were finally dialyzed against sodium carbonate solution (166 mM $NaCO_3H$, pH 8) for T22-PE24-H6 and sodium carbonate with salt solution (166 mM $NaCO_3H$, 333 mM NaCl, pH 8) for T22-GFP-H6. Protein purity was determined by Sodium Dodecyl Sulfate Polyacrylamide Gel Electrophoresis (SDS-PAGE) and Western blot immunodetection with anti-H6 monoclonal antibody (Santa Cruz Biotechnology). Protein integrity was assessed by Matrix-Assisted Laser Desorption Ionization Time-of-Flight (MALDI-TOF) mass spectrometry. Final protein concentration was determined by Bradford assay. DNA content was determined using the formula% DNA = (11.6R - 6.32)/(2.16-R), considering R = A260/A280 ratio.

2.3. Manufacturing of secretory microgranule and lyophilization

The manufacture of secretory microgranules followed methods as previously described [41]. $ZnCl_2$ was used as a divalent cation and cross-linking agent to interact with histidine residues in the C-terminal his-tag of both T22-GFP-H6 and T22-PE24-H6. Briefly, a molar excess of $ZnCl_2$ (diluted from a stock of 200 mM) was added to the proteins previously diluted in Milli-Q water to a final protein concentration of 2 mg/mL in 250 μL, with $ZnCl_2$ used in a molar 1:300 ratio of protein: cation. The mixtures were incubated for 10 min without agitation at room temperature, and later centrifuged in 1.5 ml eppendorf tubes at 15, 000 x g for 15 min to collect the secretory granules and separate them from the residual supernatant. The supernatant was assessed by Bradford to determine the percentage of precipitation. Secretory granules were stored at −80 °C for further use without the addition of buffer or storage solution. For lyophilization, granules were thawed and briefly resuspended by pipetting up-and-down in 100 μL of Buffers 1–4 (compositions available on Fig. 3) to act as protective buffering conditions to endure lyophilization. Granules that were lyophilized without buffer (WB) were equally thawed and received no manipulation. All samples were prepared for lyophilization in a biosafety cabin, and then frozen for 2 h at −80 °C. The lyophilization process was carried out in 1.5 ml Eppendorf tubes that were left open and covered with Parafilm pierced 6–8 times per tube. Frozen Eppendorf tubes were placed in a Lyophilizer LyoQuest (Telstar) previously stabilized for temperature and vacuum conditions, and the process was carried out during 16 h under vacuum levels lower than 0.05 mbar. Granules C were not lyophilized as control.

2.4. Release of soluble protein from secretory microgranules

Quantification of protein release from secretory microgranules was performed in triplicate using a spectrophotometric method. All granules (irrespective of lyophilization or downstream processing) were resuspended in 250 μL of protein storage solution (granule C and WB) or Milli-Q water (granules B1-B4), as schematized in Fig. 3. Buffers 1–4 were prepared with 20 mM Citrate pH 6 and varying percentages of additives, as follows: buffer 1 (4% Trehalose); buffer 2 (4% Trehalose, 0.01% Polysorbate 80), buffer 3 (8 % Trehalose, 0.01% Polysorbate 80) and buffer 4 (6% Trehalose 0.04% Polysorbate 80). Resuspended granules were then incubated at 37 °C without agitation for time frames varying from 7 to 30 days. At each time point, samples were briefly centrifuged to collect all drops from the lid and granules were resuspended by pipetting up-and-down 10 times. 50 μL were taken from each sample and centrifuged for 10 min at 15 000 × g at 4 °C to isolate soluble and insoluble fractions. Soluble protein was then quantified in triplicate in a NanoDrop One System (Thermo Scientific) and plotted.

2.5. Size measurement by dynamic light scattering

Size measurements of the intensity and volume size distribution of T22-GFP-H6 and T22-PE24-H6 were performed by Dynamic Light Scattering (DLS) at 25 °C and 633 nm in a Zetasizer Nano ZS (Malvern Instruments Limited). All samples were measured in 5 replicates. Only values obtained by intensity are presented in the graphs, and only samples presenting a concentration > 0.1 mg/ml were measured.

2.6. Determination of specific fluorescence

For fluorimetry assays, soluble T22-GFP-H6 was diluted in buffers 1–4 and compared to T22-GFP-H6 released from granules lyophilized in the presence of buffers 1–4. All samples were diluted to the same concentration before measurements. The excitation wavelength (λex) was set at 488 nm and the emission spectra collected, while the excitation slit was set at 2.5 nm and the emission slit at 5 nm. Fluorescence was measured in a Cary Eclipse Fluorescence Spectrophotometer (Agilent Technologies) in a quartz cell with a 10 mm path of light.

2.7. Electron microscopy

For high-resolution electron microscopy, drops of 10 μL of each sample at 0.3 mg/mL were deposited on silicon wafers (Ted Pella Inc.) and air dried overnight. The images of the secretory microgranules, lyophilized or not, were obtained using field emission scanning electron microscopy (FESEM Zeiss Merlin) operating at 2 kV and equipped with a high-resolution secondary electron detector. Representative images were obtained at a wide range of high magnifications.

2.8. Cell culture and internalization assay

CXCR4+ cervical cancer cell lines (HeLa ATCC—CCL-2) were used to study the activity of secretory microgranules in vitro. Cells were routinely cultured in Minimum Essential Medium (Mem Alpha Medium 1X + GlutaMAX™), supplemented with 10 % fetal bovine serum (FBS and incubated in a humidified atmosphere at 37 °C and 5 % of CO_2. For internalization assays, HeLa cells were cultured in 24-well plates in its medium until 70 % confluence was reached. The medium was then exchanged for OptiPRO Serum Free Medium before the addition of T22-GFP-H6 in granules or in soluble form. Protein uptake was determined at 24 h at a final concentration of 100 nM. Cells were detached, and external bound protein was removed by Trypsin-EDTA at 1 mg/mL exposure for 15 min at 37 °C. Intracellular protein fluorescence was determined by flow cytometry using a CytoFLEX (Beckman Coulter) with blue laser (488 nm). The resultant data were processed by a CytExpert software. In addition, the internalization specificity through the CXCR4 receptor was tested by exposing cells to the CXCR4 antagonist AMD3100 1 h prior to protein incubation at a 1:10 ratio (protein/AMD3100). The displayed relative fluorescence values were obtained by dividing the intracellular fluorescence values under each condition by

the background fluorescence values of non-exposed control cells in the same experiment.

2.9. Cell viability assays

For cell viability assays, human CXCR4$^+$cancer cell lines HeLa (cervical cancer, ATCC—CCL-2), Toledo (diffuse large B cell lymphoma, ATCC—CRL-2631™) and UM-SSC-22A-CXCR4$^+$ (head and neck squamous carcinoma kindly provided by Dr. Gregory Oakley and subsequently transfected with CXCR4-Luciferase lentiviral plasmid) [61] were used [61,62]. The HeLa cell line was grown in previously described conditions. For viability assays, cells were cultured in opaque-walled 96-well plates at a final concentration of 3500 cells per well for 24 h until 70 % confluence was reached. Granules and soluble proteins were incubated at different concentrations for 48 h using MEM Alpha GlutaMAX medium. Toledo cells were initially grown in RPMI 1640 medium supplemented with 10 % FBS, 1 % Glutamine, 1 % StrepPen and seeded at a final concentration of 27,000 cells per well, being maintained in a 5 % CO_2 humidified atmosphere. For HeLa and Toledo cell viability experiments, we followed the commercial recommended protocol using CellTiter-Glo Luminescent Cell Viability Assay (Promega), measuring results in a Multilabel Plate Reader Victor3 (Perkin Elmer). For UM-SSC-22A CXCR4$^+$, a similar protocol was performed, but cells were initially grown in Dulbecco's Modified medium (DMEM High Glucose) supplemented with 10 % FBS, 1 % Glutamine, 1 % StrepPen and seeded at a final concentration of 5000 cells per well, being maintained in a 10 % CO_2 humidified atmosphere. In this case, the cell viability assay was performed using the colorimetric cell proliferation kit II (XTT, Roche Diagnostic), following supplier instructions (4 h of incubation). Results were measured in a Multilabel Plate Reader Victor 3 (Perkin Elmer).

2.10. Statistical analysis

Statistical significance was analyzed using GraphPad Prism 8.0.2. We employed one-way ANOVA followed by a Tukey post-test for T22-GFP-H6 cell viability experiments. For experiments carried out with AMD3100 to measure specificity, we used an unpaired t-test. For protein release assays, significance was determined by two-way ANOVA followed by Bonferroni post-test. Significance was established (*) when $p < 0.05$. For IC50 the significance was expressed in terms of the confidence interval of 99 %, calculated using GraphPad Prism.

3. Results

For the construction of the model secretory granules, we have selected here T22-GFP-H6 and T22-PE24-H6 (Figure 2A), both being modular proteins of biomedical interest in oncology and therefore with potential clinical application. The structure of the core domains in these multifunctional proteins is very different (Fig. 2A) and this fact prevents any bias or structure-influenced deviation of the results in the analysis of the granules. Upon production in bacteria, they assemble as oligomeric, nearly DNA-free nanoparticles with negative Z potential and sizes of around 16 and 111 nm respectively (Figure 2A). These proteins attach to and internalize into CXCR4-overexpressing cells, through the highly precise binding of the peptide T22 to the cell surface chemokine receptor CXCR4 [63–66]. This molecule is an important marker in prognosis, diagnosis and therapy in oncology [67–70]. Because of the proper folding and biological activities of GFP (fluorescence) and PE24 (a cytotoxic fragment of the *Pseudomonas aeruginosa* exotoxin), the systemic administration of these constructs in animal models of CXCR4$^+$ cancers causes either the selective fluorescent enlightening of the tumor and metastatic foci [66] or the selective destruction of tumoral cells and tissues [71,72]. In the presence of a molar excess of divalent cations, they form micro-scale aggregates [33] with potential as protein drug depots [33], with a molecular architecture and protein leakage capabilities similar to those of endocrine secretory granules (Figure 2B). Usually, His-tagged proteins are released from these granules in the form of oligomeric nanomaterials (Figure 2B), whose multivalence, envisaging biomedical applications, is very appropriate for cooperative receptor binding and cellular uptake [73,74].

Taking the resulting granules as models, we wanted to explore how lyophilization (Fig. 3), the preferred storage approach for protein drugs [49], might affect the protein leakage profile of these materials and, also, the conformational and functional quality of the products once released. A negative impact would of course preclude further scaling up development and transfer to the pharma sector of these and other clinically appealing proteins formulated as secretion materials. For that, variations of a citrate buffer with trehalose and polysorbate 80 (B1-B4), one of the most used formulations for the lyophilization of protein drugs [75,76], have been explored (Fig. 3). In contrast to alternative buffers, citrate is appreciated for its wide pH working range (typically 3.0–6.2 [56]), and trehalose and polysorbate for their capability to stabilize the native structure of biological systems in extreme environments, including lyophilization [77,78]. Appropriate controls in which protein samples were lyophilized without buffer (WB) or not lyophilized (C) were also included (Fig. 3).

In a first look, the level of hydration of the granules upon lyophilization, visually interpreted through their powder-like or paste-like appearance, seemed to be highly dependent on the buffer used (Fig. 4A). The samples processed directly from precipitated, non-resuspended material (WB) were estimated to retain, visually, less water than the others did. The formation of a proper lyophilized cake, beyond being an anecdotal issue, is relevant because the condition of the material and its level of hydration may impact its functionality, as well as to contribute to decreased preservation. Under electron microscopy observation (Fig. 4B), the WB material showed a rougher surface compared with buffer-treated versions, that exhibited a smooth patinated surface. No clear difference was observed among granules prepared with different compositions of excipients (buffers B1–4), with a size range moving between approximately 10 and 50 μm.

At this point, we wanted to explore how de-hydration treatment might have impacted the endocrine-like functionalities of the materials. When protein release from buffer-treated granules was tested compared with fresh (C) material, not submitted to lyophilization/reconstitution, WB samples of both proteins showed a reduced leakage, indicating, in this case, a narrower availability of the embedded protein (Fig. 5). In contrast and surprisingly, all types of citrate buffer used for lyophilization/reconstitution allowed the release of amounts of T22-GFP-H6 or T22-PE24-H6 higher than the those leaked from the control C sample (Fig. 5). Despite the slight variability observed in the observed leaking profiles, the impact of specific buffers over the amount of released protein was highly coincident when comparing the two model proteins, with B4 being the optimal (Fig. 5). This observation was suggestive of a consistent buffer-controlled protein leakage rather than data scattering.

In all the conditions under which protein release was detected, the size of the leaked T22-GFP-H6 was determined by intensity to be around 15 nm, and slightly higher in the case of T22-PE24-H6, both with expected and moderate polydispersion indexes (Fig. 6A). This was indicative, as expected, of oligomeric nanosized versions reached or maintained by the proteins once solubilized. It is noteworthy that some buffer compositions, such as B1 and B2, induced the release of nanoparticles with deviations from the expected size. In this regard, it must be noted that a precise multimeric supramolecular architecture (isometric, virus-like organization) reached by the present (and other) nanoparticles might be necessary or highly convenient for refined functions such as cell targeting and internalization [79]. Therefore, uncontrolled variations in such defined organization occurring in the downstream processing/storage of biomaterials is undesirable. Downstream and storage comprise a set of processes that should primarily preserve the specialized activities of such smart materials. Interestingly, the fluorimetry spectra of the released protein revealed a more

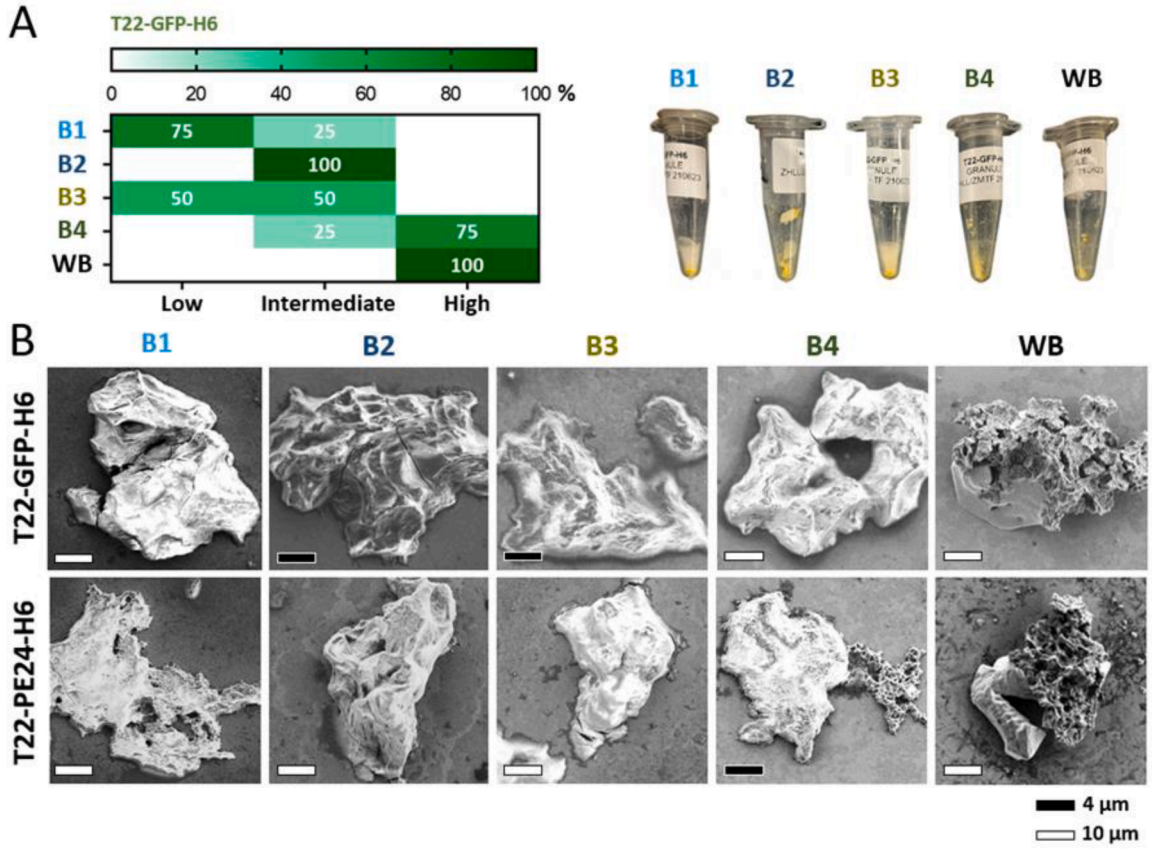

Fig. 4. Hydration and morphology of lyophilized granules. (A) Qualitative analysis of lyophilized cakes regarding their visual aspect. Pictures depict representative images of granules lyophilized without buffer (WB) or prepared with different buffer compositions, depicting the powdery level of lyophilized cakes, ranging from high (completely powdery) to low (hygroscopic). (B) FESEM micrographs showing randomly picked granules lyophilized under different conditions.

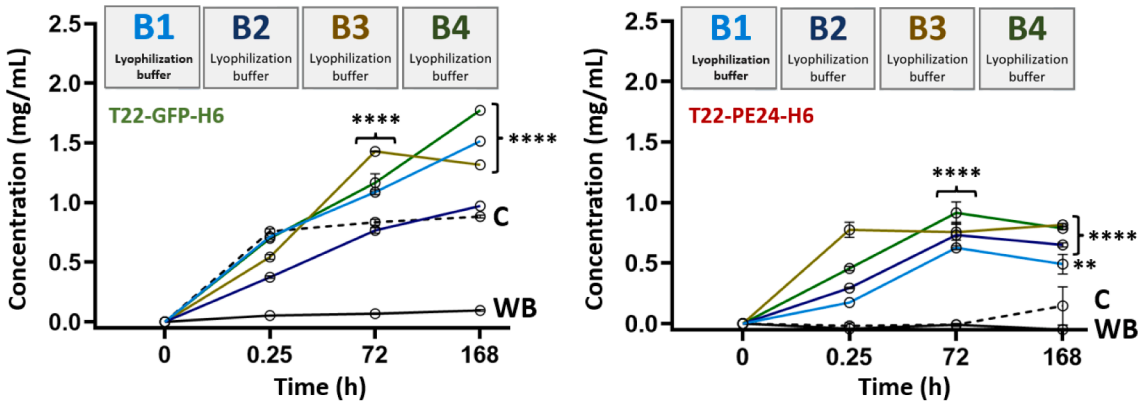

Fig. 5. Protein release from lyophilized granules. SDS-PAGE based quantification of T22-GFP-H6 and T22-PE24-H6 released from secretory granules lyophilized without any downstream processing (WB), in comparison with control granules (C) that were not lyophilized. Also, the SDS-PAGE based quantification of T22-GFP-H6 and T22-PE24-H6 released from secretory granules lyophilized after their preparation in different buffers B1-B4 is shown, in comparison with the control granules (C). Data are expressed as mean ± SEM, $n = 3$. Statistical comparisons in relation to C and/or WB (****$p < 0.0001$ or **$p < 0.01$). Slight decreases in the amount of soluble released proteins can be due to their precipitation during the analysis.

consistent tertiary structure in the released protein when compared to the soluble building blocks (freshly purified polypeptides) used for the generation of the granules (both compared in the same buffer and dilution). Therefore, the aggregation of the proteins as secretory granules resulted in a detectable structural stabilization that was retained upon protein release (Fig. 6B).

In the context of the previous data and to finely examine the properties of the citrate buffer that are relevant to the endocrine-like function of the materials, we adjusted and tested both the pH and citrate concentration (starting from the optimal formulation of B4) in a comparative way. As a first observation, B4 was able to recover and even to maximize the secretory capabilities of C and WB materials formed by either protein (Fig. 7A). This fact indicated that the loss of endocrine-like functions observed in WB was reversible, and that the protein-leaking capabilities of the fresh C materials can be improved just by the selection of a proper buffer. The decrease observed for some samples

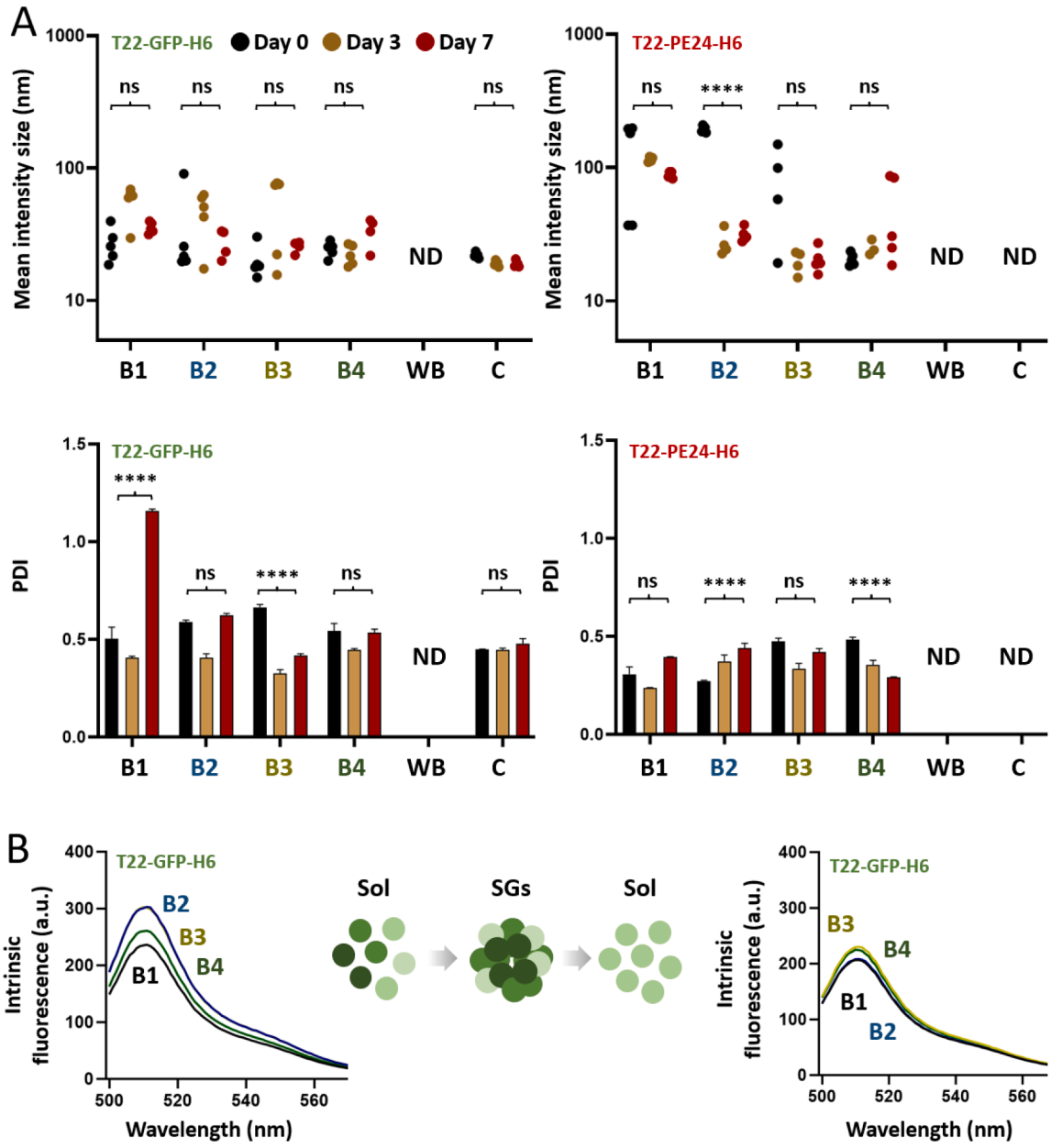

Fig. 6. Characterization of nanoparticles released from granules lyophilized under different conditions. (A) DLS plots representing measurements of the hydrodynamic size of nanoparticles released from granules at different time points. ND stands for not detectable and the term is used for samples in which insufficient nanoparticle was released to perform a reliable size measurement. The average polydispersion (PDI) index is shown at the bottom, for each condition and time. (B) Fluorimeter spectra of T22-GFP-H6 comparing nanoparticles diluted in buffers 1–4 (left) and nanoparticles released from secretory granules lyophilized in buffers 1–4 (right). The scheme represents how the heterogeneity of nanoparticle fluorimeter intensity in different buffer compositions is reduced when nanoparticles are incorporated in SG and later released. All samples were adjusted to be assessed in the same concentration. Data expressed as mean ± SEM, $n = 3$. Statistical comparisons between time 0 and 7 days were done for each sample (****$p < 0.0001$).

may be due to protein precipitation either during the incubation at 37 °C or analysis. Then, citrate buffer is a regulatory agent that can modulate protein release irrespective of the process step when it is added to the granules, either before or after lyophilization, acting even on non-lyophilized granules. Also, the specific combination of pH 6 and citrate was clearly optimal to enhance protein release (Fig. 7B), while citrate was clearly active in assisting disintegration only above 10 nM (Fig. 7C). It must be noted that, using PBS pH 6, the acidic pH, *per se*, was not able to regulate protein leakage and that citrate was necessary. Interestingly, these experiments were performed with citrate buffer without any additives (trehalose or polysorbate 80). This observation confirmed that citrate, but not other elements of the buffer formulation is responsible for the secretory control.

Finally, the biological activity of the lyophilized endocrine-like granular system was explored over cell culture. Testing the biological activity of the model polypeptides was especially necessary since conformational arrangements of the protein submitted to aggregation and disaggregation events had been observed (Fig. 6B). First, by using versions of the T22-GFP-H6-based material, we assessed that the granular particles were not intrinsically toxic upon exposure to HeLa cultured cells (Fig. 8A). After 24 h of exposure and upon a harsh trypsin treatment, the fluorescence of T22-GFP-H6 was detected inside the cells. This uptake was inhibited by AMD3100 (Fig. 8B), a selective antagonist of CXCR4 that specifically blocks T22-CXCR4 interactions [80–82]. This

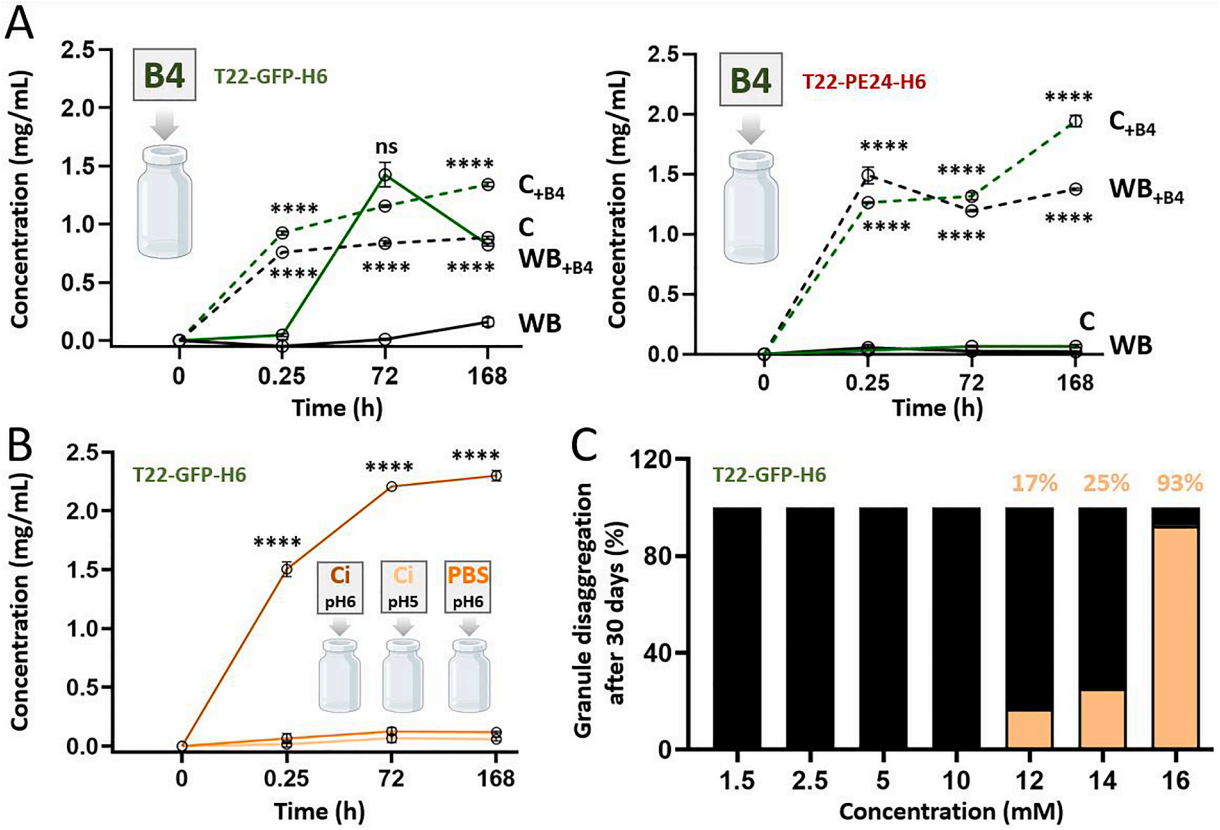

Fig. 7. Impact of citrate buffers on protein release. (A) Impact of the addition of Buffer 4 at different steps of downstream processing. Protein release was measured by SDS-PAGE for secretory granules that were lyophilized without buffer (WB) or not lyophilized (control – C) and received B4 only in the final step of reconstitution of lyophilized granules, in comparison with WB and C reconstituted in carbonate storage solution. (B) Evaluation of the impact of acidic pH on protein release over 7 days. Protein released was quantified in granules lyophilized without buffer (WB) and reconstituted in citrate buffer in different pH (5.0 or 6.0), in comparison with PBS pH 6.0. (C) Quantification by Nanodrop, expressed in percentage, of total protein released vs retained from secretory granules at day 30, comparing granules lyophilized without buffer (WB) and reconstituted in citrate buffer with molarities from 1.5 to 16 mM. Data expressed as mean ± SEM, $n = 3$. Statistical comparisons in relation to C and WB for panel A and Ci-pH5 and PBS-pH6 for panel B (****$p < 0.0001$ or *$p < 0.05$). Slight decreases in the amount of soluble released proteins can be due to their precipitation during the analysis.

fact demonstrated the expected performance of T22, displayed on the surface of the released nanoparticles, in promoting CXCR4-mediated cell internalization. In a similar way, the cytotoxicity of T22-PE24-H6 released from microparticles in HeLa cells was also inhibited when AMD3100 was added to the cell culture media as a competitor (Fig. 8C). The CXCR4-dependent cytotoxicity of T22-PE24-H6, representative of its therapeutic potential as a targeted anticancer drug, was further evaluated and fully assessed in three different patient-derived cancer cells lines, namely HeLa (cervical cancer), UM-SSC-22A-CXCR4$^+$ (head and neck squamous cell carcinoma) and Toledo (diffuse large B cell lymphoma) (Fig. 8D-F, respectively). Again, in this particular study, citrate was required for a proper performance of the released material, matching that of the soluble protein freshly recovered from recombinant bacteria. Again, WB samples showed a reduced cytotoxicity, as highlighted in the table presented in Fig. 8G. Such a level of cell death probably resulted from a residual CXCR4-dependent effect of the whole granules over cells rather than to a precise activity of the released protein. In this context, protein release from this material was not detected in previous experiments (Fig. 3).

4. Discussion

Synthetic secretory granules, resulting from metal-his coordination, are emerging platforms for time-prolonged protein drug delivery [33,83], with clinical applications in oncology [33], regenerative medicine [40], immunization [84] and antimicrobial therapies [41]. Being mimetics of secretory granules in mammals that store and deliver peptide and protein hormones [21,28], their sustained endocrine-like protein release is linked to the spontaneous and slow disintegration process undergone by such microparticles under physiological conditions [36]. As dynamic protein depots, their subcutaneous administration makes possible a steady supply of biologically functional protein for a few weeks [33,38]. This fact, in a clinical setting, is expected to minimize the undesired drug level oscillations (peak and valley) associated to the systemic administration of soluble, conventional drugs [85,86]. However, so far, the kinetics and extent of protein release from the granular system have been reluctant to rational engineering, with the selection of the clustering cation being the only possibility of relatively rough control [38]. Such a cation-dependent modulation of protein release is due to the different coordination strengths shown by metals according to the Irving-William series [87], and the relative easiness of protein detachment provided by each of the possible clustering agents.

In the present study, we have explored whether lyophilization could be an appropriate protocol envisaging the long-term storage of these materials in compliance with industrial demands and transfer, and clinically oriented large-scale handling. If so, a proper formulation of the lyophilization buffer should also be set to ensure not only the functionality of the clustered building block proteins but also the capability to be detached from the granules, under physiological conditions, and through kinetics compatible with prolonged drug release purposes. Since citrate combined with sugar is a preferred media for drug lyophilization [88], and citrate buffers are very well-known stabilizers of

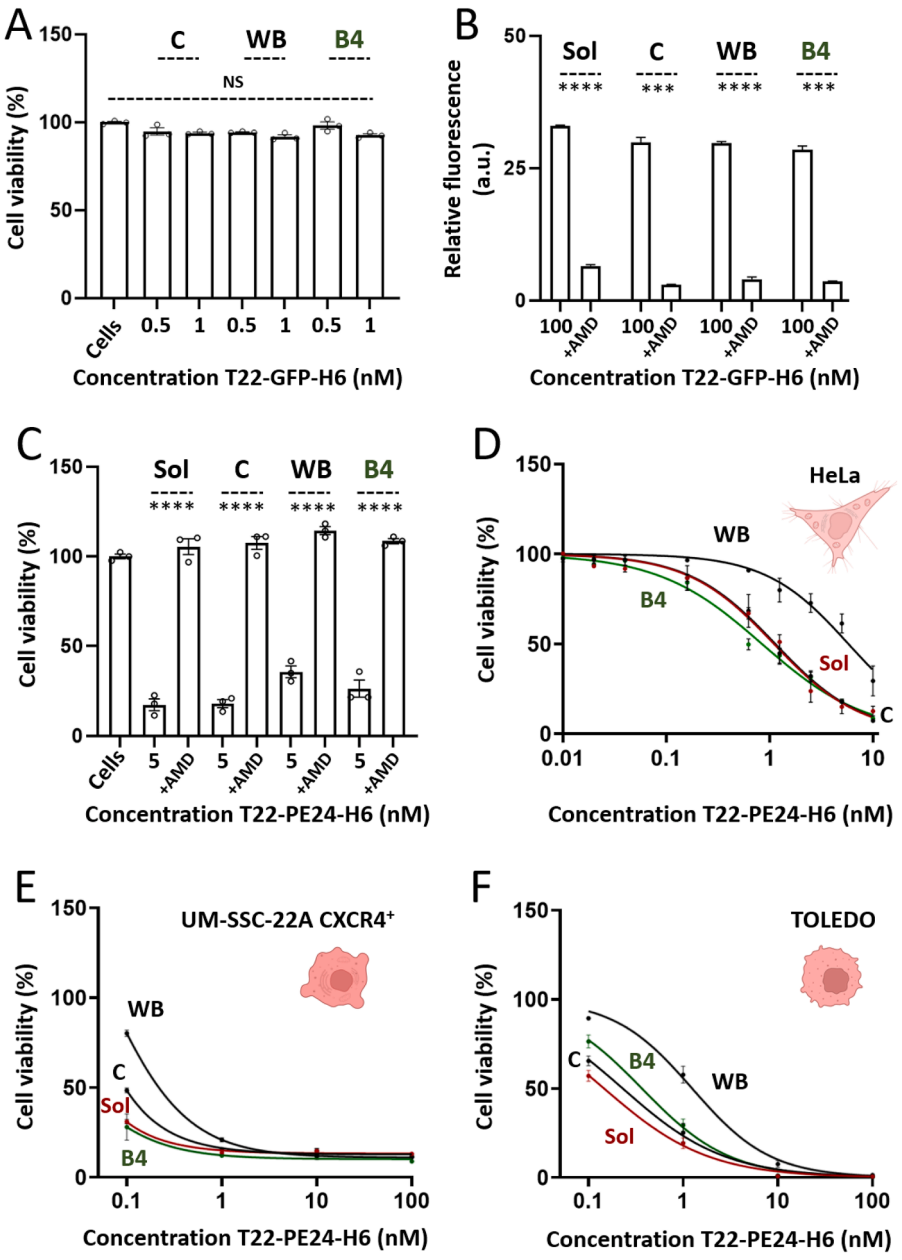

G

Cell line		Soluble	Control	WB	B4
HeLa	IC_{50} (nm)	1.10	1.14	5.78	0.84
	99% CI	0.87 to 1.36	0.87 to 1.45	4.45 to 8.05	0.68 to 1.03
UM-SSC-22A-CXCR4+	IC_{50} (nm)	< 0.1	< 0.1	0.34	< 0.1
	99% CI	-	-	0.19 to 0.60	-
TOLEDO	IC_{50} (nm)	0.15	0.23	1.25	0.37
	99% CI	0.11 to 0.20	0.15 to 0.34	0.90 to 1.72	0.27 to 0.50

(caption on next page)

Fig. 8. Functionality of protein released from secretory granules. SOL represents the soluble protein, C refers to control non-lyophilized granules, WB refers to granules lyophilized without buffer and B4 stands for granules lyophilized after downstream preparation in buffer 4. (A) Cell viability measured in HeLa cells after exposure to different concentrations of T22-GFP-H6 granules prepared in different conditions, for 48 h. (B) Internalization and CXCR4-specificity of T22-GFP-H6 in HeLa cells, assessing if this process remains specific to CXCR4 receptors after downstream processing of granules. Protein internalization was quantified after 24 h incubation in the presence of 100 nM of granules or soluble protein, using AMD3100 as a CXCR4-antagonist that blocks cell binding and internalization through CXCR4. Arbitrary units of fluorescence (au) were used, as described in Methods section (C) HeLa cell viability and CXCR4-specificity of T22-PE24-H6. Cell survival was quantified after 48 h incubation in the presence of 5 nM of granules or soluble protein, using AMD3100 as an antagonist. (D) HeLa cell viability when exposed to T22-PE24-H6 granules prepared using different downstream steps and soluble protein at different concentrations for48 h. (E) UM-SSC-22A-CXCR4$^+$ cell viability when exposed to T22-PE24-H6 granules prepared using different downstream steps and soluble protein at different concentrations for 48 h. (F) Toledo cell viability when exposed to T22-PE24-H6 granules prepared using different downstream steps and soluble protein at different concentrations for 48 h. (G) Table summarizing the IC_{50} of T22-PE24-H6 in the different presentations and cell lines assessed in panels d-F. Data expressed as mean ± SEM, $n = 3$. Statistical comparisons in relation to cells for panel A and presence of AMD for panels B and C (****$p < 0.0001$ or ***$p < 0.001$).

protein conformation [89], we performed our testing using variations in a citrate buffer formulation [78–80]. According to the obtained data, the use of this buffer largely stabilizes, from structural and functional points of view, the secretory microparticles formed by two modular proteins validated in oncology and used here as models, namely T22-GFP-H6 and T22-PE24-H6 (Figs. 6A-B). Such stabilization and further secretory performance require a precise combination of citrate and pH 6, while pH 5 is already nonfunctional (Fig. 7B) and citrate concentrations below 10 nM are also nonfunctional (Fig. 7C). From 12 to 16 nM, the extent of disintegration and the consequent protein release can be finely regulated (Fig. 7C). Importantly, the use of an appropriate citrate buffer is not only keeping and stabilizing the therapeutic protein within the granules (Fig. 6B) but it is also recovering the secretory and functional properties of granules lyophilized in the absence of buffer, and thus biologically inactive (Fig. 7A). Under these conditions, the embedded protein is effectively released for at least 30days (Fig. 7C), in the form of stable nanoparticles (Fig. 6A), that keep the fluorescence (for T22-GFP-H6), cytotoxicity (for T22-PE24-H6) or selective cell targeting (both) of the building blocks (Figs. 8A-C). Importantly, the protein nanoparticles, upon release, are fully functional and perform as expected in cell culture (by either illuminating or killing CXCR4$^+$ cells in a CXCR4-dependent fashion), in absence of unexpected intrinsic toxicity of either released protein or granular depots (Fig. 8A-F). The action of the released protein is clearly observed two days after the addition of the granules to the culture media, a time by which an important fraction of the material has already disassembled (Figs. 5 and 7A). The role of sodium citrate in the enhancement and in the fine regulation of the endocrine-like functionalities might be related to its chelating properties [59,60,90] that make it routinely used as a chelating agent [91]. Thus, the presence of citrate in the granules stimulates protein leakage, which would be the result of moderate chelation plus conformational changes undergone within the aggregates (Fig. 6B) and assisted by the buffer components. From a separate point of view, the above buffers and handling conditions are routinary and lack structural or methodological complexity. Also, the procedures proposed here are compliant with industrial demands and needs. Therefore, since lyophilization is a preferred storage form for protein drugs [92,93] and aligned with the long term lyophilization technology roadmap for industrial precompetitive research and development [94], the approach proposed here opens clear clinical possibilities for artificial secretory granules in oncology [34], vaccinology [81], tissue engineering [95] and antimicrobials [41], among others. Of course, the sensitivity of particular protein species to lyophilization might restrict the universal applicability of the platform, although this storage method is particularly friendly for proteins and protein drugs, to which it has been adapted during decades of development in the biopharma industry [96]. As an additional checkpoint, it must be noted that the Zn-assisted aggregation as endocrine-like protein clusters has His as a preferred residue for cation binding [97], and ideally, the target proteins must contain His clusters consisting of a few residues. The number of His residue in these clusters critical for precipitation has not been finely determined, but previous analyses have observed that the close occurrence of 2–3 His is sufficient for Zn-mediated cross-linking [98].

The present study is limited to two model proteins. However, the obtained data are sufficient to assertively prove lyophilization as a suitable method for the storage, in a functional form, of a new and intriguing type of protein materials intended for the time-prolonged delivery of protein drugs in vivo. It must be noted that the structural differences between the core parts of the modular T22-GFP-H6 and T22-PE24-H6 (Fig. 2), even though they do not guarantee the universality of the approach, are sufficient to dismiss the utility of lyophilization as restricted to a single and very particular conformation. Considering the potency of protein drugs and relevance of protein-based drugs in the BioPharma industry [99–101], the identification of lyophilization as a convenient preservation method is a step forward the clinical development of synthetic, protein secretory granules for endocrine-like, time prolonged protein delivery.

5. Conclusions

We have determined a lyophilization protocol suited to the stable storage and effective reconstitution of synthetic secretory granules, thus enabling the transfer of this platform to the industrial sector. It is also a step further towards the regulatory route aiming at the development and implementation of drugs based on this emerging time-prolonged drug delivery system. Additionally, we have identified physicochemical parameters that allow a very fine and robust control of the protein release profile. Lyophilization in a standard citrate-sugar buffer not only keeps protein stability, but it enhances secretion compared to control hydrated granules (Fig. 7A). On the other hand, variations of citrate concentration, at pH 6, tightly regulate the endocrine-like profile, offering not only a preservation tool but also an unexpectedly useful mechanism for the design and regulation of the dynamism of protein release from the granular depots.

CRediT authorship contribution statement

Marianna TP Favaro: Writing – review & editing, Methodology, Investigation, Data curation, Conceptualization. **Hèctor López-Laguna:** Writing – review & editing, Methodology, Investigation, Formal analysis, Data curation, Conceptualization. **Eric Voltà-Durán:** Writing – review & editing, Methodology, Investigation. **Lorena Alba-Castellon:** . **Julieta M. Sánchez:** Writing – review & editing, Methodology, Investigation. **Isolda Casanova:** Resources, Methodology, Investigation. **Ugutz Unzueta:** Writing – review & editing, Supervision, Methodology, Conceptualization. **Ramón Mangues:** Funding acquisition. **Antonio Villaverde:** Writing – original draft, Supervision, Resources, Conceptualization. **Esther Vázquez:** Writing – review & editing, Supervision, Project administration, Funding acquisition, Conceptualization.

Declaration of competing interest

The authors declare the following financial interests/personal relationships which may be considered as potential competing interests: HLL, JMS, RM, AV and EV have a patent application PROTEIN NANO OR MICROPARTICLES AS ARTIFICIAL INCLUSION BODIES (PCT/EP2020/

059994)under negotiation for license. The other authors declare that they have no known competing financial interests or personal relationships that could have appeared to influence the work reported in this paper.

Data availability

Raw data can be found on https://doi.org/10.34810/data1196.

Acknowledgments

We appreciate the support from AEI (Spain) for the development of multimeric recombinant drugs (PID2019–105416RB-I00/AEI/10.13039/501100011033 and PDC2022–133858-I00 to E.V., and PID2022–1368450 OB-10/AEI/10.13039/501100011033 to AV and EV) and to Instituto de Salud Carlos III (PI20/00400 and PI23/00318 to U.U., and PI21/00150 to R.M.) co-funded by European Regional Development Fund (ERDF, a way to make Europe). JMS is supported with a María Zambrano postdoctoral researcher contract (677904) from Ministerio de Universidades and European Union ("Financed by European Union-Next GenerationEU").The authors also appreciate the financial support received from AGAUR (2021SGR00092 to A.V. and 2021SGR01140 to R.M), from CIBER -Consorcio Centro de Investigación Biomédica en Red- (CB06/01/0014 and CB06/01/1031), Instituto de Salud Carlos III, Ministerio de Ciencia e Innovación, through intramural projects (NANO4CANCER to A.V.,NANOREMOTE to E.V. and 4NANOMETS to R.M.). U.U. is supported by Miguel Servet contract (CP19/00028) from ISCIII co-funded by European Social Fund (ESF investing in your future), L. A-C is supported by AECC (Spain) Postdoctoral fellowship (POSTD20070ALBA). We also acknowledge the support from Microscopy Service, the Proteomics and Structural Biology Service and the Cell Culture, Antibody Production and Cytometry Service, all in the UAB. Protein production was partially performed by the ICTS "NANBIOSIS", more specifically by the Protein Production Platform of CIBER in Bioengineering, Biomaterials & Nanomedicine (CIBER-BBN)/ IBB, at the UAB (http://www.nanbiosis.es/portfolio/u1-protein-production-platform-ppp/).

References

[1] D. Mishra, K. Glover, S. Gade, R. Sonawane, T. Raghu Raj Singh, Safety, biodegradability, and biocompatibility considerations of long-acting drug delivery systems, in: Long-Acting Drug Delivery Systems: Pharmaceutical, Clinical, and Regulatory Aspects, 2021. 10.1016/B978-0-12-821749-8.00008-2.
[2] N. Kutner, K.R. Kunduru, L. Rizik, S. Farah, Recent advances for improving functionality, biocompatibility, and longevity of implantable medical devices and deliverable drug delivery systems, Adv. Funct. Mater. 31 (2021), https://doi.org/10.1002/adfm.202010929.
[3] H. Park, K. Park, Biocompatibility issues of implantable drug delivery systems, Pharm. Res. 13 (1996), https://doi.org/10.1023/A:1016012520276.
[4] D.S. Kohane, R. Langer, Biocompatibility and drug delivery systems, Chem. Sci. (2010) 1, https://doi.org/10.1039/c0sc00203h.
[5] M. Karvekar, A.B. Khan, A brief review on sustained release matrix type drug delivery system, J. Pharma. Res. 16 (2017), https://doi.org/10.18579/jpcrkc/2017/16/3/118769.
[6] S. Diksha, D. Dhruv, D.N. Prasad, H. Mansi, Sustained release drug delivery system with the role of natural polymers: a review, J. Drug Deliv. Therapeut. 9 (2019), https://doi.org/10.22270/jddt.v9i3-s.2859.
[7] M. Vigata, C. Meinert, D.W. Hutmacher, N. Bock, Hydrogels as drug delivery systems: a review of current characterization and evaluation techniques, Pharmaceutics 12 (2020), https://doi.org/10.3390/pharmaceutics12121188.
[8] H. Idrees, S.Z.J. Zaidi, A. Sabir, R.U. Khan, X. Zhang, S.U. Hassan, A review of biodegradable natural polymer-based nanoparticles for drug delivery applications, Nanomaterials 10 (2020), https://doi.org/10.3390/nano10101970.
[9] W.B. Liechty, D.R. Kryscio, B.V. Slaughter, N.A. Peppas, Polymers for drug delivery systems, Annu. Rev. Chem. Biomol. Eng. 1 (2010), https://doi.org/10.1146/annurev-chembioeng-073009-100847.
[10] J. Li, D.J. Mooney, Designing hydrogels for controlled drug delivery, Nat. Rev. Mater. 1 (2016), https://doi.org/10.1038/natrevmats.2016.71.
[11] H. Abdelkader, Z. Fathalla, A. Seyfoddin, M. Farahani, T. Thrimawithana, A. Allahham, A.W.G. Alani, A.A. Al-Kinani, R.G. Alany, Polymeric long-acting drug delivery systems (LADDS) for treatment of chronic diseases: inserts, patches, wafers, and implants, Adv. Drug. Deliv. Rev. 177 (2021) 113957, https://doi.org/10.1016/j.addr.2021.113957.
[12] V.L. Mehta, N. Chatterjee, Drug delivery systems: past, present and future, J. Int. Med. Sci. Acad. 8 (1995), https://doi.org/10.2174/1389450043345407.
[13] A. Balistreri, E. Goetzler, M. Chapman, Functional amyloids are the rule rather than the exception in cellular biology, Microorganisms 8 (2020), https://doi.org/10.3390/microorganisms8121951.
[14] S.A. Levkovich, E. Gazit, D. Laor Bar-Yosef, Two decades of studying functional amyloids in microorganisms, Trend. Microbiol. 29 (2021), https://doi.org/10.1016/j.tim.2020.09.005.
[15] N. Van Gerven, S.E. Van der Verren, D.M. Reiter, H. Remaut, The role of functional amyloids in bacterial virulence, J. Mol. Biol. 430 (2018), https://doi.org/10.1016/j.jmb.2018.07.010.
[16] M.S. Rubel, S.A. Fedotov, A.V. Grizel, J.V. Sopova, O.A. Malikova, Y.O. Chernoff, A.A. Rubel, Functional mammalian amyloids and amyloid-like proteins, Life 10 (2020), https://doi.org/10.3390/life10090156.
[17] A.V. Sergeeva, A.P. Galkin, Functional amyloids of eukaryotes: criteria, classification, and biological significance, Curr. Genet. 66 (2020), https://doi.org/10.1007/s00294-020-01079-7.
[18] M. Spiess, N. Beuret, C. Prescianotto Baschong, J. Rutishauser, Amyloid-like aggregation of provasopressin, in: Vitam Horm, 2020. https://doi.org/10.1016/bs.vh.2019.08.014.
[19] G. Cereghetti, S. Saad, R. Dechant, M. Peter, Reversible, functional amyloids: towards an understanding of their regulation in yeast and humans, Cell Cycle 17 (2018), https://doi.org/10.1080/15384101.2018.1480220.
[20] L.P. Blanco, M.L. Evans, D.R. Smith, M.P. Badtke, M.R. Chapman, Diversity, biogenesis and function of microbial amyloids, Trends Microbiol. (2012) 20, https://doi.org/10.1016/j.tim.2011.11.005.
[21] S.K. Maji, M.H. Perrin, M.R. Sawaya, S. Jessberger, K. Vadodaria, R.A. Rissman, P. S. Singru, K.P.R. Nilsson, R. Simon, D. Schubert, D. Eisenberg, J. Rivier, P. Sawchenko, W. Vale, R. Riek, Functional amyloids as natural storage of peptide hormones in pituitary secretory granules, Science 325 (1979) 328–332, https://doi.org/10.1126/SCIENCE.1173155/SUPPL_FILE/MAJI.SOM.PDF (2009).
[22] C. Seuring, J. Verasdonck, J. Gath, D. Ghosh, N. Nespovitaya, M.A. Wälti, S. K. Maji, R. Cadalbert, P. Güntert, B.H. Meier, R. Riek, The three-dimensional structure of human β-endorphin amyloid fibrils, Nat. Struct. Mol. Biol. 27 (2020), https://doi.org/10.1038/s41594-020-00515-z.
[23] A. Soragni, S.K. Maji, R. Riek, Toward a comprehension of functional aggregation into amyloids in pituitary secretory granules, Amyloid 17 (2010), https://doi.org/10.1021/acsami.3c08643.
[24] S. Takahashi, Immunocytochemical and immuno-electron-microscopical study of growth hormone cells in male and female rats of various ages, Cell Tissue Res. 266 (1991), https://doi.org/10.1007/BF00318183.
[25] W.C. Hymer, W.J. Kraemer, Resistance exercise stress: theoretical mechanisms for growth hormone processing and release from the anterior pituitary somatotroph, Eur. J. Appl. Physiol. 123 (2023), https://doi.org/10.1007/s00421-023-05263-8.
[26] P.S. Dannies, Prolactin and growth hormone aggregates in secretory granules: the need to understand the structure of the aggregate, Endocr. Rev. (2012) 33, https://doi.org/10.1210/er.2011-1002.
[27] P.S. Dannies, Mechanisms for storage of prolactin and growth hormone in secretory granules, Mol. Genet. Metab. 76 (2002), https://doi.org/10.1016/S1096-7192(02)00011-2.
[28] R.S. Jacob, S. Das, S. Ghosh, A. Anoop, N.N. Jha, T. Khan, P. Singru, A. Kumar, S. K. Maji, Amyloid formation of growth hormone in presence of zinc: relevance to its storage in secretory granules, Sci. Rep. 6 (2016) 1–18, https://doi.org/10.1038/srep23370, 20161 6.
[29] D. Chatterjee, R.S. Jacob, S. Ray, A. Navalkar, N. Singh, S. Sengupta, L. Gadhe, P. Kadu, D. Datta, A. Paul, A. Sakunthala, S. Mehra, C. Pindi, S. Kumar, P.S. Singru, S. Senapati, S.K. Maji, Co-aggregation and secondary nucleation in the life cycle of human prolactin/galanin functional amyloids, Elife 11 (2022). 10.7554/eLife.73835.
[30] A. Hoffman, D. Stepensky, Pharmacodynamic aspects of modes of drug administration for optimization of drug therapy, Crit. Rev. Ther. Drug. Carrier Syst. 16 (1999), https://doi.org/10.1615/critrevtherdrugcarriersyst.v16.i6.20.
[31] P.J. Crowley, L.G. Martini, Formulation design: new drugs from old, Drug Discov. Today Ther. Strateg. 1 (2004), https://doi.org/10.1016/j.ddstr.2004.11.020.
[32] A. Hoffman, Pharmacodynamic aspects of sustained release preparations, Adv. Drug. Deliv. Rev. 33 (1998), https://doi.org/10.1016/S0169-409X(98)00027-1.
[33] J.M. Sánchez, H. López-Laguna, P. Álamo, N. Serna, A. Sánchez-Chardi, V. Nolan, O. Cano-Garrido, I. Casanova, U. Unzueta, E. Vazquez, R. Mangues, A. Villaverde, Artificial inclusion bodies for clinical development, Adv. Sci. 7 (2020), https://doi.org/10.1002/advs.201902420.
[34] J.M. Sánchez, H. López-Laguna, E. Parladé, A. Di Somma, A.L. Livieri, P. Álamo, R. Mangues, U. Unzueta, A. Villaverde, E. Vázquez, Structural stabilization of clinically oriented oligomeric proteins during their transit through synthetic secretory amyloids, Adv. Sci. (2024), https://doi.org/10.1002/advs.202309427.
[35] H. López-Laguna, J.M. Sánchez, J.V. Carratalá, M. Rojas-Peña, L. Sánchez-García, E. Parladé, A. Sánchez-Chardi, E. Voltà-Durán, N. Serna, O. Cano-Garrido, S. Flores, N. Ferrer-Miralles, V. Nolan, A. de Marco, N. Roher, U. Unzueta, E. Vazquez, A. Villaverde, Biofabrication of functional protein nanoparticles through simple His-tag engineering, ACS Sustain. Chem. Eng. 9 (2021), https://doi.org/10.1021/acssuschemeng.1c04256.
[36] E. Parladé, J.M. Sánchez, H. López-Laguna, U. Unzueta, A. Villaverde, E. Vázquez, Protein features instruct the secretion dynamics from metal-supported synthetic amyloids, Int. J. Biol. Macromol. 250 (2023) 126164, https://doi.org/10.1016/J.IJBIOMAC.2023.126164.

[37] N. Serna, A. Falgàs, A. García-León, U. Unzueta, Y. Núñez, A. Sánchez-Chardi, C. Martínez-Torró, R. Mangues, E. Vazquez, I. Casanova, A. Villaverde, Time-prolonged release of tumor-targeted protein–MMAE nanoconjugates from implantable hybrid materials, Pharmaceutics 14 (2022), https://doi.org/10.3390/pharmaceutics14010192.

[38] P. Álamo, E. Parladé, H. López-Laguna, E. Voltà-Durán, U. Unzueta, E. Vazquez, R. Mangues, A. Villaverde, Ion-dependent slow protein release from in vivo disintegrating micro-granules, 28 (2021) 2383–2391. 10.1080/10717544.2021.1998249.

[39] L. Bosch-Camós, C. Martínez-Torró, H. López-Laguna, J. Lascorz, J. Argilaguet, A. Villaverde, F. Rodríguez, E. Vázquez, Nanoparticle-based secretory granules induce a specific and long-lasting immune response through prolonged antigen release, Nanomaterials 14 (2024) 435, https://doi.org/10.3390/nano14050435.

[40] N. Serna, O. Cano-Garrido, J.M. Sánchez, A. Sánchez-Chardi, L. Sánchez-García, H. López-Laguna, E. Fernández, E. Vázquez, A. Villaverde, Release of functional fibroblast growth factor-2 from artificial inclusion bodies, (2020). 10.1016/j.jconrel.2020.08.007.

[41] N. Serna, H. López-Laguna, P. Aceituno, M. Rojas-Peña, E. Parladé, E. Voltà-Durán, C. Martínez-Torró, J.M. Sánchez, A. Di Somma, J.V. Carratalá, A.L. Livieri, N. Ferrer-Miralles, E. Vázquez, U. Unzueta, N. Roher, A. Villaverde, Efficient delivery of antimicrobial peptides in an innovative, slow-release pharmacological formulation, Pharmaceutics 15 (2023) 2632, https://doi.org/10.3390/pharmaceutics15112632.

[42] L. Jorgensen, S. Hostrup, E.H. Moeller, H. Grohganz, Recent trends in stabilising peptides and proteins in pharmaceutical formulation - considerations in the choice of excipients, Expert. Opin. Drug. Deliv. 6 (2009), https://doi.org/10.1517/17425240903199143.

[43] M.E. Krause, E. Sahin, Chemical and physical instabilities in manufacturing and storage of therapeutic proteins, Curr. Opin. Biotechnol. 60 (2019), https://doi.org/10.1016/j.copbio.2019.01.014.

[44] C. Mueller, U. Altenburger, S. Mohl, Challenges for the pharmaceutical technical development of protein coformulations, J. Pharma. Pharmacol. 70 (2018), https://doi.org/10.1111/jphp.12731.

[45] L.M. Pandey, Physicochemical factors of bioprocessing impact the stability of therapeutic proteins, Biotechnol. Adv. 55 (2022), https://doi.org/10.1016/j.biotechadv.2022.107909.

[46] M. Akbarian, S.H. Chen, Instability challenges and stabilization strategies of pharmaceutical proteins, Pharmaceutics 14 (2022), https://doi.org/10.3390/pharmaceutics14112533.

[47] M. Bjelošević, A. Zvonar Pobirk, O. Planinšek, P. Ahlin Grabnar, Excipients in freeze-dried biopharmaceuticals: contributions toward formulation stability and lyophilisation cycle optimisation, Int. J. Pharm. 576 (2020), https://doi.org/10.1016/j.ijpharm.2020.119029.

[48] A. M, Lyophilisation of protein-based drugs, Ceska a Slovenska Farmacie 63 (2014).

[49] E.V. Blynskaya, S.V. Tishkov, K.V. Alekseev, Technological approaches to improving the process lyophilization of protein and peptide drugs, Russ. J. Biotherap. 16 (2017), https://doi.org/10.17650/1726-9784-2017-16-1-6-11.

[50] D. Jain, S.S. Mahammad, P.P. Singh, R. Kodipyaka, A review on parenteral delivery of peptides and proteins, Drug Dev. Ind. Pharm. 45 (2019), https://doi.org/10.1080/03639045.2019.1628770.

[51] A.D. Stephens, N. Nespovitaya, M. Zacharopoulou, C.F. Kaminski, J.J. Phillips, G. S. Kaminski Schierle, Different structural conformers of monomeric α-synuclein identified after lyophilizing and freezing, Anal. Chem. 90 (2018), https://doi.org/10.1021/acs.analchem.8b01264.

[52] A.I.P. Taylor, P.J. Davis, L.D. Aubrey, J.B.R. White, Z.N. Parton, R.A. Staniforth, Simple, reliable protocol for high-yield solubilization of seedless amyloid-β monomer, ACS Chem. Neurosci. 14 (2023), https://doi.org/10.1021/acschemneuro.2c00411.

[53] D.B. Teplow, Preparation of amyloid β-protein for structural and functional studies, Methods Enzymol. (2006) 413, https://doi.org/10.1016/S0076-6879(06)13002-5.

[54] C. Wu, S. Shamblin, D. Varshney, E. Shalaev, Advance understanding of buffer behavior during lyophilization, in: Lyophilized Biologics and Vaccines, Springer New York, New York, NY, 2015: pp. 25–41. https://doi.org/10.1007/978-1-4939-2383-0_3.

[55] T.J. Zbacnik, R.E. Holcomb, D.S. Katayama, B.M. Murphy, R.W. Payne, R. C. Coccaro, G.J. Evans, J.E. Matsuura, C.S. Henry, M.C. Manning, Role of buffers in protein formulations, J. Pharm. Sci. 106 (2017) 713–733, https://doi.org/10.1016/J.XPHS.2016.11.014.

[56] B. Susrisweta, L. Veselý, R. Štůsek, A. Hauptmann, T. Loerting, D. Heger, Investigating freezing-induced acidity changes in citrate buffers, Int. J. Pharm. 643 (2023) 123211, https://doi.org/10.1016/J.IJPHARM.2023.123211.

[57] P. Manju, A. Babu, S.P. S, D. Tirumalarao, P.V. A, V.B. Kamble, D. Jaiswal-Nagar, Variation of citrate to metal cation ratio for dense and phase pure $BaZrO_3$ via autocombustion synthesis, J. Amer. Ceram. Soc. 105 (2022) 5082–5101, https://doi.org/10.1111/jace.18477.

[58] Z. karimi, M. Goli, The effect of chelating agents including potassium tartrate and citrate on the maximum reduction of lead and cadmium during soaking and cooking from some different varieties of rice available in Iran, Food. Sci. Nutr. 9 (2021) 5112–5118, https://doi.org/10.1002/fsn3.2473.

[59] J.W. Baynes, D.B. Murray, The metal chelators, trientine and citrate, inhibit the development of cardiac pathology in the zucker diabetic rat, Exp. Diabetes Res. 2009 (2009) 1–6, https://doi.org/10.1155/2009/696378.

[60] B. Francis, C. Seebart, I.I. Kaiser, Citrate is an endogenous inhibitor of snake venom enzymes by metal-ion chelation, Toxicon 30 (1992) 1239–1246, https://doi.org/10.1016/0041-0101(92)90440-G.

[61] E. Rioja-Blanco, I. Arroyo-Solera, P. Álamo, I. Casanova, A. Gallardo, U. Unzueta, N. Serna, L. Sánchez-García, M. Quer, A. Villaverde, E. Vázquez, R. Mangues, L. Alba-Castellón, X. León, Self-assembling protein nanocarrier for selective delivery of cytotoxic polypeptides to CXCR4+ head and neck squamous cell carcinoma tumors, Acta. Pharm. Sin. B 12 (2022) 2578–2591, https://doi.org/10.1016/j.apsb.2021.09.030.

[62] A. Falgàs, V. Pallarès, U. Unzueta, M.V. Céspedes, I. Arroyo-Solera, M.J. Moreno, A. Gallardo, M.A. Mangues, J. Sierra, A. Villaverde, E. Vázquez, R. Mangues, I. Casanova, A CXCR4-targeted nanocarrier achieves highly selective tumor uptake in diffuse large B-cell lymphoma mouse models, Haematologica (2020) 105, https://doi.org/10.3324/haematol.2018.211490.

[63] H. Tamamura, Y. Xu, T. Hattori, X. Zhang, R. Arakaki, K. Kanbara, A. Omagari, A. Otaka, T. Ibuka, N. Yamamoto, H. Nakashima, N. Fujii, A low-molecular-weight inhibitor against the chemokine receptor CXCR4: a strong anti-HIV peptide T140, Biochem. Biophys. Res. Commun. 253 (1998), https://doi.org/10.1006/bbrc.1998.9871.

[64] T. Murakami, T. Nakajima, Y. Koyanagi, K. Tachibana, N. Fujii, H. Tamamura, N. Yoshida, M. Waki, A. Matsumoto, O. Yoshie, T. Kishimoto, N. Yamamoto, T. Nagasawa, A small molecule CXCR4 inhibitor that blocks T cell line-tropic HIV-1 infection, J. Experim. Med. 186 (1997), https://doi.org/10.1084/jem.186.8.1389.

[65] T. Murakami, T.-Y. Zhang, Y. Koyanagi, Y. Tanaka, J. Kim, Y. Suzuki, S. Minoguchi, H. Tamamura, M. Waki, A. Matsumoto, N. Fujii, H. Shida, J. A. Hoxie, S.C. Peiper, N. Yamamoto, Inhibitory mechanism of the CXCR4 antagonist T22 against human immunodeficiency virus type 1 infection, J. Virol. 76 (2002), https://doi.org/10.1128/jvi.76.2.933.2002.

[66] U. Unzueta, M.V. Céspedes, N. Ferrer-Miralles, I. Casanova, J. Cedano, J. L. Corchero, J. Domingo-Espín, A. Villaverde, R. Mangues, E. Vázquez, Intracellular CXCR4+ cell targeting with T22-empowered protein-only nanoparticles, Int. J. Nanomed. 7 (2012) 4533–4544, https://doi.org/10.102147/IJN.S34450.

[67] B. Furusato, A. Mohamed, M. Uhlén, J.S. Rhim, CXCR4 and cancer: review Article, Pathol. Int. 60 (2010), https://doi.org/10.1111/j.1440-1827.2010.02548.x.

[68] M. Kircher, P. Herhaus, M. Schottelius, A.K. Buck, R.A. Werner, H.J. Wester, U. Keller, C. Lapa, CXCR4-directed theranostics in oncology and inflammation, Ann. Nucl. Med. 32 (2018), https://doi.org/10.1007/s12149-018-1290-8.

[69] Y. Gao, C. Li, M. Nie, Y. Lu, S. Lin, P. Yuan, X. Sun, CXCR4 as a novel predictive biomarker for metastasis and poor prognosis in colorectal cancer, Tumor. Biol. 35 (2014), https://doi.org/10.1007/s13277-013-1545-x.

[70] H. Zhao, L. Guo, H. Zhao, J. Zhao, H. Weng, B. Zhao, CXCR4 over-expression and survival in cancer: a system review and meta-analysis, Oncotarget 6 (2015), https://doi.org/10.18632/oncotarget.3217.

[71] Y. Núñez, A. Garcia-León, A. Falgàs, N. Serna, L. Sánchez-García, A. Garrido, J. Sierra, A. Gallardo, U. Unzueta, E. Vázquez, A. Villaverde, R. Mangues, I. Casanova, T22-PE24-H6 nanotoxin selectively kills CXCR4-high expressing AML patient cells in vitro and potently blocks dissemination in vivo, Pharmaceutics (2023) 15, https://doi.org/10.3390/pharmaceutics15030727.

[72] Z. Zhao, Y. Huang, J. Wang, H. Lin, F. Cao, S. Li, Y. Li, Z. Li, X. Liu, A self-assembling CXCR4-targeted pyroptosis nanotoxin for melanoma therapy, Biomater. Sci. 11 (2023) 2200–2210, https://doi.org/10.1039/D2BM02026B.

[73] A. Barnard, D.K. Smith, Self-assembled multivalency: dynamic ligand arrays for high-affinity binding, Angewandte Chemie - Int. Ed. 51 (2012), https://doi.org/10.1002/anie.201200076.

[74] C. Dalal, A. Saha, N.R. Jana, Nanoparticle multivalency directed shifting of cellular uptake mechanism, J. Phys. Chem. C (2016) 120, https://doi.org/10.1021/acs.jpcc.5b11059.

[75] W. Wang, Lyophilization and development of solid protein pharmaceuticals, Int. J. Pharm. 203 (2000), https://doi.org/10.1016/S0378-5173(00)00423-3.

[76] A. Arsiccio, R. Pisano, The Preservation of lyophilized human growth hormone activity: how do buffers and sugars interact? Pharm. Res. 35 (2018) https://doi.org/10.1007/s11095-018-2410-9.

[77] Q. Zhang, B. Liu, J. Chong, L. Ren, Y. Zhao, X. Yuan, Combination of hydrophobically modified γ-poly(glutamic acid) and trehalose achieving high cryosurvival of RBCs, Sci. China. Technol. Sci. 64 (2021) 806–816, https://doi.org/10.1007/s11431-020-1549-2.

[78] M.B. Gelb, K.M.M. Messina, D. Vinciguerra, J.H. Ko, J. Collins, M. Tamboline, S. Xu, F.J. Ibarrondo, H.D. Maynard, Poly(trehalose methacrylate) as an excipient for insulin stabilization: mechanism and safety, ACS Appl. Mater. Interf. 14 (2022) 37410–37423, https://doi.org/10.1021/acsami.2c09301.

[79] U. Unzueta, M.V. Céspedes, E. Vázquez, N. Ferrer-Miralles, R. Mangues, A. Villaverde, Towards protein-based viral mimetics for cancer therapies, Trends Biotechnol. (2015) 33, https://doi.org/10.1016/j.tibtech.2015.02.007.

[80] E. De Clercq, AMD3100/CXCR4 inhibitor, Front. Immunol. 6 (2015), https://doi.org/10.3389/fimmu.2015.00276.

[81] S. Hatse, K. Princen, G. Bridger, E. De Clercq, D. Schols, Chemokine receptor inhibition by AMD3100 is strictly confined to CXCR4, FEBS Lett. 527 (2002), https://doi.org/10.1016/S0014-5793(02)03143-5.

[82] H.-Y. Kim, J.-Y. Hwang, S.-W. Kim, H.-J. Lee, H.-J. Yun, S. Kim, D.-Y. Jo, The CXCR4 antagonist AMD3100 has dual effects on survival and proliferation of myeloma cells in vitro, Cancer Res. Treat 42 (2010), https://doi.org/10.4143/crt.2010.42.4.225.

[83] T.Y. Chen, W.J. Cheng, J.C. Horng, H.Y. Hsu, Artificial peptide-controlled protein release of Zn2+-triggered, self-assembled histidine-tagged protein microparticle, Colloids Surf. B Biointerfaces 187 (2020), https://doi.org/10.1016/j.colsurfb.2019.110644.
[84] M.T.P. Favaro, P. Alamo, N. Roher, M. Chillon, J. Lascorz, M. Márquez, J. L. Corchero, R. Mendoza, C. Martínez-Torró, N. Ferrer-Miralles, L.C.S. Ferreira, R. Mangues, E. Vázquez, E. Parladé, A. Villaverde, Zinc-assisted microscale granules made of the SARS-CoV-2 spike protein trigger neutralizing, antivirus antibody responses, ACS Mater. Lett. (2024) 954–962, https://doi.org/10.1021/acsmaterialslett.3c01643.
[85] S. Ummadi, B. Shravani, N.G.R. Rao, M.S. Reddy, B. Sanjeev, Overview on controlled release dosage forms, Int. J. Pharma. Sci. 3 (2013).
[86] S. Karna, S. Chaturvedi, V. Agrawal, M. Alim, Formulation approaches for sustained release dosage forms: a review, Asian J. Pharma. Clin. Res. 8 (2015).
[87] H. Irving, R.J.P. Williams, The stability of transition-metal complexes, J. Chem. Soc. (Resumed) (1953), https://doi.org/10.1039/jr9530003192.
[88] C. Wu, S. Shamblin, D. Varshney, E. Shalaev, Advance understanding of buffer behavior during lyophilization, in: Lyophilized Biologics and Vaccines, 2015. 10.1007/978-1-4939-2383-0_3.
[89] S. O.Ugwu, S. P.Apte, The effect of buffers on protein conformational stability, Pharma. Technol. 81 (2004).
[90] J.P. Glusker, Citrate conformation and chelation: enzymatic implications, Acc. Chem. Res. 13 (1980), https://doi.org/10.1021/ar50154a002.
[91] P. Sivagurunathan, S.R. Gibin, Preparation and characterization of nickel ferrite nano particles by co-precipitation method with citrate as chelating agent, J. Mater. Sci. 27 (2016), https://doi.org/10.1007/s10854-015-4065-1.
[92] A. Butreddy, K.Y. Janga, S. Ajjarapu, S. Sarabu, N. Dudhipala, Instability of therapeutic proteins — An overview of stresses, stabilization mechanisms and analytical techniques involved in lyophilized proteins, Int. J. Biol. Macromol. 167 (2021), https://doi.org/10.1016/j.ijbiomac.2020.11.188.
[93] R.L. Remmele, S. Krishnan, W.J. Callahan, Development of stable lyophilized protein drug products, Curr. Pharm. Biotechnol. 13 (2012), https://doi.org/10.2174/138920112799361990.
[94] A. Alexeenko, E. Topp, Future directions: lyophilization technology roadmap to 2025 and beyond, in: Drying Technologies for Biotechnology and Pharmaceutical Applications, 2020. 10.1002/9783527802104.ch15.
[95] H. López-Laguna, P.M. Tsimbouri, V. Jayawarna, I. Rigou, N. Serna, E. Voltà-Durán, U. Unzueta, M. Salmeron-Sanchez, E. Vázquez, M.J. Dalby, A. Villaverde, Hybrid micro-/nanoprotein platform provides endocrine-like and extracellular matrix-like cell delivery of growth factors, ACS Appl. Mater. Interf. (2024), https://doi.org/10.1021/acsami.4c01210.
[96] J.F. Carpenter, B.S. Chang, W. Garzon-Rodriguez, T.W. Randolph, Rational design of stable lyophilized protein formulations: theory and practice, Pharm. Biotechnol. (2002) 13, https://doi.org/10.1007/978-1-4615-0557-0_5.
[97] H. López-Laguna, J. Sánchez, U. Unzueta, R. Mangues, E. Vázquez, A. Villaverde, Divalent cations: a molecular glue for protein materials trends in biochemical sciences an official publication of the international union of biochemistry and molecul ar biology, Trends Biochem. Sci. 45 (2020), https://doi.org/10.1016/j.tibs.2020.08.003.
[98] H. López-Laguna, R. Cubarsi, U. Unzueta, R. Mangues, E. Vázquez, A. Villaverde, Endosomal escape of protein nanoparticles engineered through humanized histidine-rich peptides, Sci. China. Mater. 63 (2020), https://doi.org/10.1007/s40843-019-1231-y.
[99] M. Muttenthaler, G.F. King, D.J. Adams, P.F. Alewood, Trends in peptide drug discovery, Nat. Rev. Drug Discov. 20 (2021), https://doi.org/10.1038/s41573-020-00135-8.
[100] K. Sharma, K.K. Sharma, A. Sharma, R. Jain, Peptide-based drug discovery: current status and recent advances, Drug Discov. Today 28 (2023), https://doi.org/10.1016/j.drudis.2022.103464.
[101] A.A. Halwani, Development of pharmaceutical nanomedicines: from the bench to the market, Pharmaceutics 14 (2022), https://doi.org/10.3390/pharmaceutics14010106.